Critical analysis of methods to estimate the fraction of absorbed or intercepted photosynthetically active radiation from ground measurements: Application to rice crops

Wenjuan Li, Hongliang Fang, Shanshan Wei, Marie Weiss, Frédéric Baret

Critical analysis of methods to estimate the fraction of absorbed or intercepted photosynthetically active radiation from ground measurements: application to rice crops

Wenjuan Li[a,b,c*], Hongliang Fang[a,b], Shanshan Wei[a,b], Marie Weiss[c] and Fréderic Baret[c]

[a]LREIS, Institute of Geographic Sciences and Natural Resources Research, Chinese Academy of Sciences, Beijing 100101, China,

[b]College of Resources and Environment, University of Chinese Academy of Sciences, Beijing 100049, China

[c]INRAE, Avignon Université, UMR 1114 EMMAH, UMT CAPTE, F-84000, Avignon, France

*Corresponding author

Highlights

- fIPAR is a good proxy of fAPAR when the background is dark as in most rice crops.
- Impact of illumination conditions and non-green components was analyzed.
- Green fAPAR can be estimated from canopy fAPAR and the GAI/PAI ratio.
- Downward DHP is recommended when estimating green fIPAR.

Abstract

Continuous and accurate ground measurements of the fraction of absorbed (fAPAR) or intercepted (fIPAR) photosynthetically active radiation by green canopy components is important to monitor canopy functioning. fAPAR and fIPAR are sensitive to illumination conditions and non-green components during the senescence stage. While several methods have been developed to estimate fAPAR or fIPAR in the field from different methods including AccuPAR, LAI-2200 and Digital Hemispheric Photograph Photography (DHP), the differences among these methods still need more investigations. The principles on which they are based are first reviewed with due attention to the assumptions used and approximations made. Two field campaigns conducted in 2012 and 2013 in northeastern China over paddy rice fields were then used to compare fAPAR and fIPAR measured using AccuPAR, DHP and LAI-2200. Results demonstrated that considering only canopy light transmittance (fIPAR), measured with AccuPAR, DHP or LAI-2200, is a good proxy of fAPAR which is computed from AccuPAR measurements of the four fluxes of the radiation balance. However, when canopy is senescing, downward looking DHP method is recommended since it is the only method that directly measures the light intercepted by green elements. Methods based on upward looking (DHP upward, AccuPAR, LAI-2200) cannot distinguish between the green and senescent vegetation elements. Corrections based on independent measurements of the ratio of the green area index (GAI) to the plant area index (PAI) (GAI/PAI) need to be used in this case, while assuming that green and senescent elements are well mixed in the canopy volume. Downward looking DHP appears to be the preferred method for relatively short and

dense canopies such as rice since it does not disturb the canopy, it is sensitive to the green elements only and allows to simulate fIPAR for any illumination conditions.

Keywords

fAPAR; fIPAR; Green fAPAR; Green fIPAR; Paddy rice; Diffuse fraction

Nomenclature

$I_t^{\downarrow}$	Incoming downward flux measured at the top of the canopy
$I_t^{\uparrow}$	Upward flux reflected by the canopy
$I_b^{\downarrow}$	Downward fluxes measured at the bottom of the canopy
$I_b^{\uparrow}$	Upward fluxes measured at the bottom of the canopy
R_c	Canopy reflectance
R_c^{bs}	Black-sky canopy reflectance under direct illumination conditions
R_c^{ws}	White-sky canopy reflectance under diffuse illumination conditions
T	Canopy transmittance
T^{bs}	Black-sky transmittance under direct illumination conditions
T^{ws}	White-sky transmittance under diffuse illumination conditions
R_s	Soil background reflectance
R_s^{bs}	Black-sky soil reflectance under direct illumination conditions
R_s^{ws}	White-sky soil reflectance under diffuse illumination conditions
R_∞	Canopy reflectance for very dense foliage
R_{sen}	Reflectance of senescent layer
P	Canopy gap fraction
θ	Zenith angle
$G(\theta)$	Leaf projection function
$\Omega(\theta)$	Canopy clumping index
DOY	Day of Year
ESU	Elementary Sampling Units
DHP	Digital Hemispherical Photography
PAR	Photosynthetically Active Radiation

f	Fraction of diffuse PAR in total PAR
fAPAR	Fraction of Absorbed PAR
$\mathrm{fAPAR}_{\mathrm{T}}$	fAPAR measured from the two-stream method using transmittance only
$\mathrm{fAPAR}^{\mathrm{bs}}$	Black-sky fAPAR under direct illumination conditions
$\mathrm{fAPAR}^{\mathrm{ws}}$	White-sky fAPAR under diffuse illumination conditions
$\mathrm{fAPAR}_{\mathrm{T}}^{\mathrm{bs}}$	Black-sky fAPAR measured from the two-stream method
$\mathrm{fAPAR}_{\mathrm{T}}^{\mathrm{ws}}$	White-sky fAPAR measured from the two-stream method
fIPAR	Fraction of Intercepted PAR
fIPAR(LAI-2200)	fIPAR measured from LAI-2200
$\mathrm{fIPAR}^{\mathrm{ws}}$(LAI-2200)	White-sky fIPAR measured from LAI-2200
$\mathrm{fIPAR}(\mathrm{DHP}_{\mathrm{up}})$	fIPAR measured from the upward DHP
$\mathrm{fIPAR}^{\mathrm{bs}}(\mathrm{DHP}_{\mathrm{up}})$	Black-sky fIPAR from the upward DHP
$\mathrm{fIPAR}^{\mathrm{ws}}(\mathrm{DHP}_{\mathrm{up}})$	White-sky fIPAR from the upward DHP
$\mathrm{GfIPAR}(\mathrm{DHP}_{\mathrm{down}})$	fIPAR of green canopy components measured from the downward DHP
$\mathrm{GfIPAR}^{\mathrm{bs}}$	Black-sky GfIPAR measured from the downward DHP
$\mathrm{GfIPAR}^{\mathrm{ws}}$	White-sky GfIPAR measured from the downward DHP
GfAPAR	fAPAR of canopy green components
$\mathrm{GfAPAR}_{\mathrm{top}}$	GfAPAR corrected from canopy fAPAR using Eq. (14)
$\mathrm{GfAPAR}_{\mathrm{mix}}$	GfAPAR corrected from canopy fAPAR using Eq. (15)
GF	Green Fraction
GAI	Green Area Index
GLAI	Green Leaf Area Index
PAI	Plant Area Index

1 Introduction

The fraction of photosynthetically active radiation (PAR, 400-700nm) absorbed by green vegetation elements (fAPAR) is closely linked to canopy functioning processes such as photosynthesis and transpiration. It also quantifies the incoming radiation available at the soil level that is mandatory for modeling soil temperature and evaporation. It is thus a key variable required in many ecosystems and crop functioning models to simulate photosynthesis and primary production (Goward and Huemmrich, 1992; McCallum et al., 2010; Monteith, 2015). fAPAR is listed as an essential climate variable (ECV) by the Global Climate Observing System (GCOS, 2016). It is often approximated by the fraction of intercepted PAR (fIPAR) because the vegetation pigments present a strong absorption in this spectral domain and the reflectivities from background are usually small for well-developed canopies (Gower et al., 1999).

Several methods have been developed to estimate fAPAR and fIPAR from ground measurements. Handheld optical devices, such as AccuPAR (Meter Group, Inc., USA), provide an efficient way to measure fAPAR under different illumination conditions (Steinberg et al., 2006). AccuPAR measures the downward and upward PAR fluxes at the top and bottom of the canopy by placing the probes above and below the canopy. Other methods such as Digital Hemispherical Photography (DHP) measure the gap fraction (upward looking) or green fraction (downward looking) to derive fIPAR in all directions. Pixel classification of the RGB images is mainly based on color contrast between leaves and the sky for the upward looking DHP to get the gap, and between green leaves and non-green elements including the background to get the green pixels for the downward looking DHP (Baret et al., 1993; Demarez et al., 2008; Leblanc et al., 2005). However, image segmentation may be affected by the illumination conditions, especially when shadows or specular reflection are observed (Fang et al., 2014a, 2018; Ye et al., 2015). LAI-2200 (LI-COR Inc., Lincoln, Nebraska, USA) measures the transmittance in the blue wavelength domain in five zenithal directions from which fIPAR can be estimated. However LAI-2200 measurements are also sensitive to the illumination conditions (Asner et al., 1998; Kobayashi et al., 2013; Leblanc and Chen, 2001). A thorough intercomparison of these instruments is still lacking.

fAPAR depends on solar zenith angle and illumination conditions, e.g., overcast or clear sky condition. The instantaneous fAPAR is highly sensitive to variations of the solar zenith angle and presents diurnal variations under clear sky conditions (Fensholt et al., 2004; Rahman et al., 2015; Zhao et al., 2018), while it shows a much smaller diurnal variations under cloudy conditions (Nouvellon, 2000; Thomas et al., 2006). The daily integrated fAPAR, which is a variable used by many canopy functioning models, has been demonstrated to be smaller under clear sky as compared to overcast conditions (Gower et al., 1999; Thomas et al., 2006). Therefore, it is required to compare the fAPAR quantities measured by different instruments under a range of illumination conditions and solar zenith angles. However, direct comparison between instruments is not always feasible due to the intrinsic properties of each device. As an example, the fAPAR measured by AccuPAR accounts for the diffuse fraction, while devices based on gap fraction measurements (DHP) may account both for the direct sunlight and the diffuse illumination. To facilitate the comparison between those different instruments, we used the decomposition proposed by Martonchik et al. (2000): fAPAR is considered as the sum of a black-sky and a white-sky components, weighted by the PAR diffuse fraction. The black-sky fAPAR, $fAPAR^{bs}$, corresponds to the direct component (collimated beam irradiance in the sun direction only) while the white-sky fAPAR, $fAPAR^{ws}$, corresponds to diffuse illumination conditions generally assumed perfectly isotropic (GCOS, 2016). Although the impact of diffuse fraction on fAPAR has been investigated (Gu et al., 2002; Jongschaap et al., 2006; Lizaso et al., 2005), few studies focused on the estimation of the black-sky and white-sky components of fAPAR or fIPAR in crops (Cohen et al., 1997; Hanan and Bégué, 1995) and none of them have intercompared the ability of the current instruments to well measure these quantities.

Since only the green photosynthetically active elements contribute directly to key processes such as photosynthesis and transpiration, green vegetation elements should be isolated to estimate fAPAR (Huemmrich et al., 2005; Pinter, 1993; Weiss et al., 2007; Xiao, 2004; Zhang et al., 2005). The presence of senescent leaves during late crop growth stages have a significant impact on fAPAR, and the relationship between fAPAR and vegetation indices (Di Bella et al., 2004; Rahman et al., 2019; Viña and Gitelson, 2005). The ground measured canopy fAPAR can be partitioned into fAPAR of green components and non-green components. Among optical instruments listed above, only downward looking DHPs allow to separate the green from the non-green elements to estimate the corresponded fraction of intercepted light. Upward looking DHPs should not be used for such a purpose since senescence often starts from the bottom layer of the crop, while the light penetrates from the top of the canopy (Baret et al., 2010). The other upward looking techniques, such as AccuPAR and LAI-2200, do not allow distinguishing between green and non-green elements. Some corrections have been proposed to consider only the green elements depending on the canopy type, either assuming that the green elements are located at the top of the canopy (Chen, 1996), or assuming that green and non-green elements are well mixed in the canopy volume (Viña and Gitelson, 2005).

The objective of this study is to compare the several methods proposed and evaluate the impact of the presence of non-green vegetation elements during the senescence phase, under different illumination conditions. For this purpose, a dedicated experiment was conducted in 2012 and 2013 where AccuPAR, DHP and LAI-2200 devices were concurrently used over paddy rice fields in northeastern China.

2 Methods

2.1 Theoretical background

2.1.1 Derivation of canopy fAPAR and fIPAR

fAPAR is calculated from the radiation balance in the PAR domain:

$$\text{fAPAR} = \frac{I_t^{\downarrow} - I_t^{\uparrow} - \left(I_b^{\downarrow} - I_b^{\uparrow}\right)}{I_t^{\downarrow}} \qquad (1)$$

where $I_t^{\downarrow}$ and $I_t^{\uparrow}$ are the downward and upward fluxes measured at the top of the canopy. $(I_b^{\downarrow} - I_b^{\uparrow})$ is the radiation absorbed by the soil background calculated as the difference between the downward ($I_b^{\downarrow}$) and upward ($I_b^{\uparrow}$) fluxes measured at the bottom of the canopy. Note that the net horizontal PAR fluxes are considered negligible as we focus on rice crops which are short canopies that do not present major heterogeneity at the scale investigated corresponding to few square meters located in an homogeneous field (Widlowski, 2010). Eq. (1) can be expressed more simply as:

$$\text{fAPAR} = 1 - R_c - T(1 - R_s) \qquad (2)$$

where $R_c = \frac{I_t^{\uparrow}}{I_t^{\downarrow}}$ is the canopy reflectance, $T = \frac{I_b^{\downarrow}}{I_t^{\downarrow}}$ is the canopy transmittance, and $R_s = \frac{I_b^{\uparrow}}{I_b^{\downarrow}}$ is the soil background reflectance in the PAR spectral domain. For short canopies such as paddy rice, it is usually difficult to measure the upward flux at the bottom of the canopy because of the short distance between the sensors and the soil surface and the large spatial heterogeneity of this flux. However, the soil background reflectance can be estimated from other independent measurements in the laboratory or over bare soils at nearby locations.

In the PAR domain, the canopy reflectance can be approximated as a linear decomposition of soil and foliage reflectance:

$$R_c \approx TR_s + (1 - T)R_{\infty} \quad (3)$$

where R_{∞} is the reflectance for very dense foliage. Combining Eqs. (2) and (3), fAPAR can be approximated using two terms:

$$fAPAR \approx (1 - T)(1 - R_{\infty}) \quad (4)$$

For dense vegetation, R_{∞} is very small ($R_{\infty} \approx 0.04$) because of the strong absorption by chlorophyll pigments in the PAR domain (Weiss et al., 2018). Therefore, Eq. (4) can be further simplified as:

$$\text{fAPAR} \approx \text{fAPAR}_{\text{T}} = 1 - T \quad (5)$$

The accuracy of this simplification depends on the fluxes reflected by the canopy and the soil background, which vary with canopy structure, illumination conditions, and background properties (Widlowski, 2010). If leaves are considered opaque, the fraction of intercepted PAR (fIPAR) can be calculated from the gap fraction P (Eq. (6)). In these conditions, P is closely approximated by canopy transmittance (T) and fIPAR ≈ fAPAR_T.

$$fIPAR = 1 - P \approx 1 - T \approx \mathrm{fAPAR}_T \quad (6)$$

2.1.2 Estimation of the canopy fAPAR and fIPAR under different illumination conditions

At a given time of the day, the total canopy fAPAR is the sum of the black-sky and white-sky fAPAR, weighted by the fraction of the incoming diffuse PAR radiation (f):

$$fAPAR = (1 - f) \cdot fAPAR^{bs} + f \cdot fAPAR^{ws} \quad (7)$$

The same black-sky and white-sky components are also defined for the fIPAR quantities. During a day, if clear-sky $fAPAR(\theta)$ and white-sky observations, $fAPAR^{ws}$, are measured, instantaneous black-sky fAPAR (fAPAR^{bs}) can be estimated based on Eq. (8):

$$fAPAR^{bs}(\theta) = \frac{fAPAR(\theta) - f(\theta) \cdot fAPAR^{ws}}{1 - f(\theta)} \quad (8)$$

Similarly, transmittance measured in the five directions by the LAI-2200 allows to compute the black-sky fIPAR, $\mathrm{fIPAR}^{bs}(\theta)$ for θ <68° by linear interpolation between the five crowns.

The fraction of intercepted black-sky PAR ($fIPAR^{bs}(\theta)$) was calculated from the green fraction (GF) for downward looking DHP or gap fraction (P) for upward looking DHP after classifying the green (downward) or sky (upward) pixels:

$$\begin{cases} FIPAR^{bs}(\theta) = GF(\theta) & \text{for downward DHP} \\ FIPAR^{bs}(\theta) = 1 - P(\theta) & \text{for upward DHP} \end{cases} \quad (9)$$

For each zenith direction, θ, with $\theta < 60°$, the green or gap fraction is averaged across all azimuthal directions from all images in an ESU to compute $GF(\theta)$ or $P(\theta)$ (Weiss and Baret, 2010). Data for $\theta > 60°$ were not considered because of the large uncertainties in the green fraction estimation due to the degraded resolution for these directions.

White-sky fIPAR ($fIPAR^{ws}$) for LAI-2200 and DHP devices can be derived by integrating $FIPAR^{bs}$ over the hemisphere (Weiss and Baret, 2010):

$$FIPAR^{ws} = 2\int_0^{\pi/2} (FIPAR^{bs}(\theta)) \cos\theta \sin\theta \, d\theta \quad (10)$$

For $\theta > 60°$ (DHP) or $\theta > 68°$ (LAI-2200), the term $(FIPAR^{bs}(\theta)) \cos\theta \sin\theta$ was approximated by linear interpolation between $\theta = 60°$ or $\theta = 68°$ and $\theta = 90°$ with $(FIPAR^{bs}(90°)) \cos 90° \sin 90° = 0$.

2.1.3 Derivation of the green fAPAR and fIPAR (GfAPAR and GfIPAR)

Assuming that all canopy elements are randomly distributed in the canopy volume, the canopy transmittance can be derived using the Poisson model (Nilson, 1971):

$$T = e^{-G(\theta)\cdot PAI\cdot\Omega(\theta)/\cos\theta} \quad (11)$$

where $G(\theta)$ is the projection function that depends on the leaf inclination distribution and direction (θ), and $\Omega(\theta)$ is the canopy clumping index. It is here assumed that $G(\theta)$ and $\Omega(\theta)$ values are the same for the green and non-green elements. The four-stream fAPAR (Eq. (2)) can then be approximated as:

$$fAPAR = 1 - R_c - (1 - R_s) \cdot e^{-G(\theta)\cdot PAI\cdot\Omega(\theta)/\cos\theta} \quad (12)$$

When there are no senescent elements, GfAPAR=fAPAR. Conversely, for canopies having senescent elements, GfAPAR can be estimated from fAPAR measurements using an independent estimate of GAI/PAI and assumptions about the distribution of the senescent elements in the canopy. When the green leaves are located at the top of the canopy above the senescent elements, Chen (1996) proposed to estimate GfAPAR using the following formulation:

$$GfAPAR^{top} = 1 - R_c - (1 - R_{sen}) \cdot e^{-G(\theta)\cdot GAI\cdot\Omega(\theta)/\cos\theta} \quad (13)$$

where R_{sen} is the reflectance of the senescent layer above the soil background. It plays the same role as R_s in Eq. (12) when there is no senescent element. Finally, GAI in Eq. (13) can be replaced by PAI in Eq. (12) using the GAI/PAI ratio:

$$GfAPAR^{top} = 1 - R_c - (1 - R_{sen}) \cdot e^{\frac{GAI}{PAI}\cdot ln(\frac{1-R_c-fAPAR}{1-R_s})} \quad (14)$$

Conversely, Viña and Gitelson (2005) assumed that the green and non-green elements are well mixed within the canopy volume, proposed the following formulation of the green fAPAR as a function of the total canopy fAPAR and the GAI/PAI ratio:

$$GfAPAR^{mix} = fAPAR \cdot GAI/PAI \qquad (15)$$

Based on the same considerations, Eqs. (14) and (15) can be applied to fIPAR values derived from upward DHP and LAI-2200 devices to get the corresponding green fIPAR, GfIPAR:

$$GfIPAR^{top} = 1 - e^{\frac{GAI}{PAI} \cdot ln(1-fIPAR)} \qquad (16)$$

$$GfIPAR^{mix} = fIPAR \cdot GAI/PAI \qquad (17)$$

Table 1 lists the fAPAR and fIPAR quantities derived from the several instruments and the associated notations and equations used. All these quantities can be computed for both black-sky and white-sky conditions.

Table 1. Quantities estimated from AccuPAR, DHP, and LAI-2200. R_c, R_s, R_{sen} and T represent the canopy reflectance, the background soil and senescent layer reflectance, and the canopy transmittance, respectively. P is the canopy gap fraction and GF is the green fraction.

Instruments	Notation	Equation	Eq. #
AccuPAR	$fAPAR(AccuPAR)$	$1 - R_c - T(1 - R_s)$	(2)
	$fAPAR_T(AccuPAR)$	$1 - T$	(5)

	$GfAPAR^{top}(AccuPAR)$	$1 - R_c - (1 - R_{sen})e^{\frac{GAI}{PAI} \cdot ln(\frac{1-R_C-fAPAR}{1-R_S})}$	(14)
	$GfAPAR^{mix}(AccuPAR)$	$fAPAR\ GAI/PAI$	(15)
Downward DHP	$GfIPAR(DHP_{down})$	GF	(9)
Upward DHP	$fIPAR(DHP_{up})$	$1 - P$	(9)
	$GfIPAR^{top}(DHP_{up})$	$1 - e^{\frac{GAI}{PAI} \cdot ln(1-fIPAR)}$	(16)
	$GfIPAR^{mix}(DHP_{up})$	$fIPAR \cdot GAI/PAI$	(17)
LAI-2200	$fIPAR(LAI - 2200)$	$1 - P$	(9)
	$GfIPAR^{top}(LAI - 2200)$	$1 - e^{\frac{GAI}{PAI} \cdot ln(1-fIPAR)}$	(16)
	$GfIPAR^{mix}(LAI - 2200)$	$fIPAR \cdot GAI/PAI$	(17)

2.2 Study area

The study area is located at the Honghe Farm (47.65° N, 133.52° E) in the Heilongjiang Province, China. The area is subjected to a humid continental monsoon climate with long and cold winter and warm, short, and humid summer. The water and soil are frozen from late October to April and thaw in late April. A single rice cultivar (*Longjing 29*) is grown in flat fields sharing the same soil properties and where the same cropping practices are applied. Rice crops are grown once a year from May to September (Fig. A1). The fields are flooded during most of the growing season.

A total of 55 Elementary Sampling Units (ESUs) of about 20 × 20 m^2 each were selected in five fields closely located and chosen to be homogeneous and similar in terms of soils and management practices. This allows to consider each ESU as representative of all the other ESUs. All ESUs were located at least at 1.5 m from the field border to limit potential edge effects. More details about the site and sampling strategy can be found in Fang et al. (2014a, 2014b).

2.3 Ground measurements

Ground measurements were carried out frequently from June 11 to September 17 in 2012, and from June 22 to August 29 in 2013 (Fig. 1). We used the “moving ESU strategy” as described by Fang et al. (2014a), considering that the measurements achieved in one ESU at a given date are representative of all the other ESUs. This allows to prevent disturbances caused by the handheld measurements along the growing season and makes destructive measurements possible. In 2012, all the measurements were taken close to sunset or under overcast conditions to estimate the white-sky fAPAR. In 2013, white-sky fAPAR was also measured near sunset or under overcast conditions and completed the same day by black-sky fAPAR measurements when the sky was clear in the morning (9:30 to 10:30 am). The field measurement dates and the corresponding solar zenith angles and diffuse fraction are shown in Fig. 1 for the several instruments considered in this study.

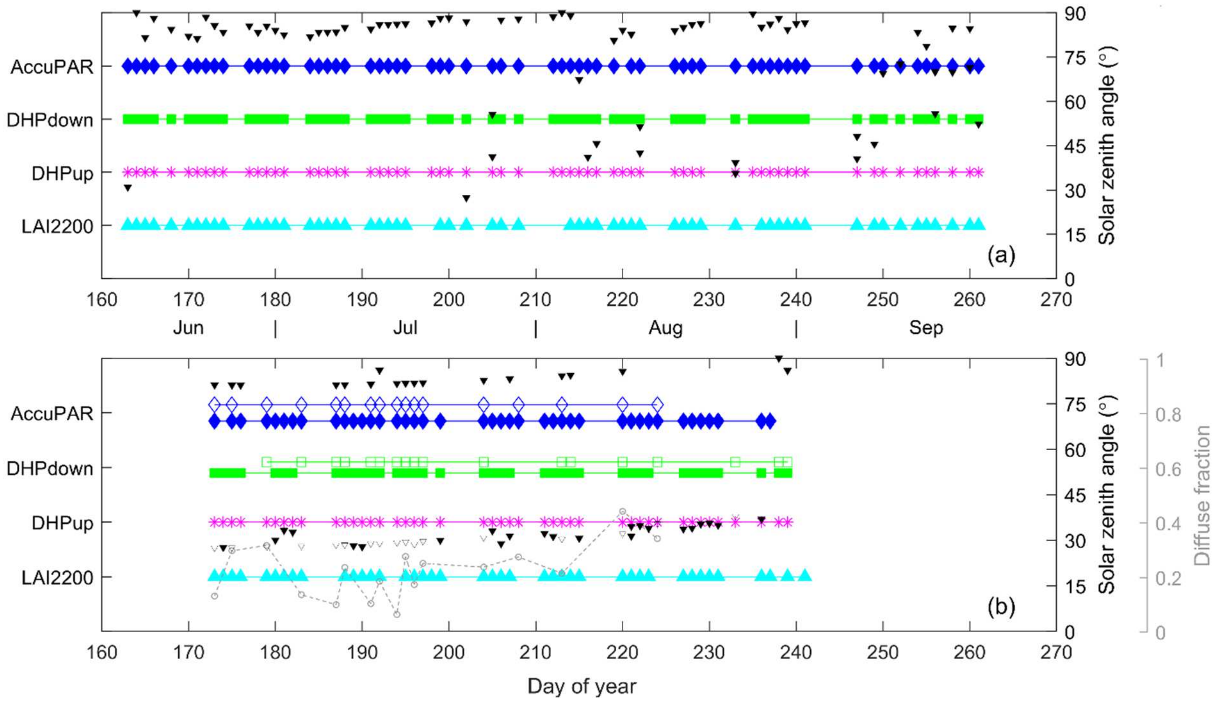

Fig. 1. Measurement dates for AccuPAR (blue diamond), DHP_{down} (green square), DHP_{up} (pink asterisk) and LAI-2200 (cyan triangle) in (a) 2012 and (b) 2013 under cloudy (filled marker) and clear (open marker, 2013) conditions. Black filled and open downward-pointing triangles represent solar zenith angles for cloudy and clear conditions (first right y-axis). Gray dashed line with open circles in (b) indicate the diffuse fraction measured for clear sky conditions in 2013 (second right y-axis).

Decagon's AccuPAR LP-80 PAR/LAI Ceptometer measures PAR using 80 individual sensors with a 180° field of view on a 1-m probe (Huemmrich et al., 2005; Senna, 2005; Steinberg et al., 2006; Thomas et al., 2006). The downward and reflected PAR fluxes at the top of canopy were measured by placing the probe approximately 1.5 m above the canopy, facing upward and downward, respectively. The canopy transmitted PAR was measured by placing the probe below the canopy looking upward. The below-canopy measurements were repeated four times in different directions to account for the row effect (Campos et al., 2017; Timlin et al., 2014; Zhong et al., 2015). The soil reflected PAR was measured twice in two different rows by placing the probe approximately 5 cm above the ground looking downward. Prior to each measurement, the AccuPAR was calibrated when the above canopy PAR was > 600 μmol/m^{2}s as recommended in the user manual (Decagon Devices, 2010). Under clear skies in 2013, the diffuse PAR was measured by blocking the direct solar illumination with a black board placed 0.5 m from the sensor. The diffuse fraction was then computed as the ratio of the diffuse to the total downward PAR. The measurement was repeated three times within one minute before, during, and after fAPAR measurements. Because the three replicates were generally consistent, their average value was considered as the diffuse fraction at the time of the fAPAR measurements.

The DHP images were taken using a Nikon D5100 camera equipped with a 4.5 mm F2.8 EX DC fisheye convertor. The DHP camera was calibrated before measurements following the CAN-EYE manual (Weiss and Baret, 2010) to obtain the optical center and the projection function of the camera and fish-eye system. The total height of the camera, including the lens, was about 16.5 cm. Two bubble levels were attached to the camera to keep it horizontal for both downward and upward measurements. In each ESU, 15 to 20 DHPs were acquired for both downward and upward directions (Fang et al., 2014a). The downward images were taken by holding the camera 0.8–1.5 m above the canopy. When the rice was higher than 70 cm, upward images were taken by placing the camera right above the background soil or water in the row. All DHP images were processed using the CAN-EYE version 6.3.3 software (https://www6.paca.inrae.fr/can-eye). Green pixels were manually separated from senescent and background pixels for the downward images during the classification step. This step was performed by the same operator throughout the season.

LAI-2200 measures the blue radiation in 5 concentric rings centered at 7°, 23°, 38°, 53° and 68°. LAI-2200 measurements were conducted always under diffuse conditions. Each measurement was repeated twice, with one above and four below canopy readings along diagonal transects between the rows. For the below canopy readings, the instrument was held about 5 cm above the background. Throughout the season, a 270° view cap was used to shield the operator. The four measurements over an ESU were averaged to obtain the mean transmittance (Fang et al., 2014a, 2014b). All AccuPAR, DHP, and LAI-2200 measurements were made within a maximum time difference of 10 minutes.

In addition to the optical measurements, canopy green area index (GAI) and plant area index (PAI) were measured in 2012 using a destructive method (Fang et al., 2014a, 2014b). Five plants were randomly harvested in the ESU and the area of green and non-green leaves, stems and ears were measured using a LI-3100C Area Meter (LI-COR, Lincoln, NE, USA). Leaf, stem, and ear area are the sum of the corresponding green and non-green measured areas. The corresponding area indices were then computed using the plant density to get the area of elements per unit ground area. GLAI corresponds to the green leaves only, while LAI includes green and non-green parts. GAI corresponds to the area of all green elements, while PAI includes the senescent parts as well.

3 Results

3.1 Dynamics of LAI, GLAI, GAI and PAI

During the rice green-up stage from sowing to the end of July (Day of year (DOY) 210), no senescence is observed: GAI and PAI are equal (Fig. 2). When the senescence starts to progress, some leaves disappear, and both PAI and GAI decrease gradually after DOY 210. Once the stems and ears are fully developed around DOY 220, their total area keep about constant. However, senescence is also progressing gradually up to almost full senescence at maturity, i.e. DOY 265 (Fig. 2). Conversely, senescence of leaves stops on DOY 240: LAI and GLAI and PAI keep about constant up to maturity, while GAI still decreases because of the senescing stems and ears. The high consistency observed between measurements across time demonstrates that the spatial variability among the several ESUs sampled was very small.

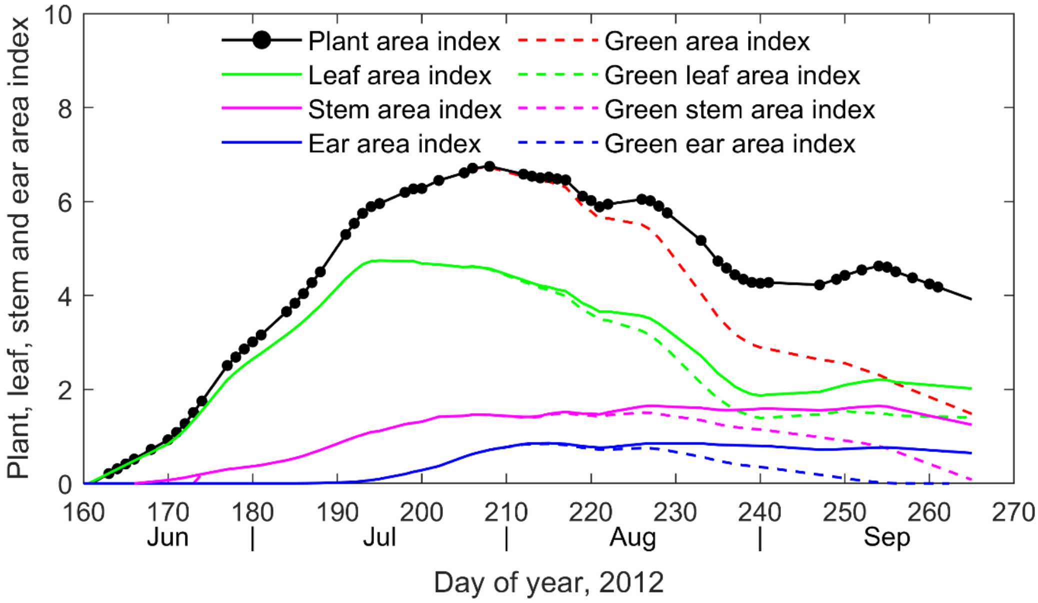

Fig. 2. Seasonal variation of plant, leaf, stem and ear area index measured by destructive method in 2012. The corresponding area of the green parts are indicated by the dashed lines. The black circles represent the actual measurements days.

3.2 fAPAR from AccuPAR

Results show that for both 2012 and 2013, canopy reflectance (R_c) is slightly higher in the beginning when the soil background is not fully covered by the vegetation, and at the end of season after the ears and senescent components began to appear. When the canopy is fully covering the soil, R_c keeps about to a low and stable value with $R_c \approx 0.04$ (Fig. 3). Soil background reflectance (R_s) shows little variation during the growing season and is low because the soil was always wet or covered by water. Canopy transmittance (T) decreases continuously from the beginning of the season until DOY 210 and then increases slightly during the senescent stage (Fig. 3) since part of the leaves are dead while another part of them show a decrease in chlorophyll, leading to an increase in leaf reflectance and transmittance in the PAR domain. Accordingly, canopy fAPAR increases from the beginning of the season up to DOY 210 and decreases during the senescent stage (Fig. 3a). The influence of the illumination conditions on the different components can be analyzed in 2013 (Fig. 3b). Canopy and soil reflectance are little impacted and remain stable. Conversely, the canopy transmittance depends on the illumination conditions mostly before DOY 210 when the canopy is not fully covering the soil. The black-sky transmittance is higher than its white-sky counterpart, and consequently the black-sky fAPAR is smaller than the white-sky fAPAR. After DOY 210, the difference between black-sky and white-sky values for both transmittance and fAPAR becomes very small due to the saturation of the canopy transmittance.

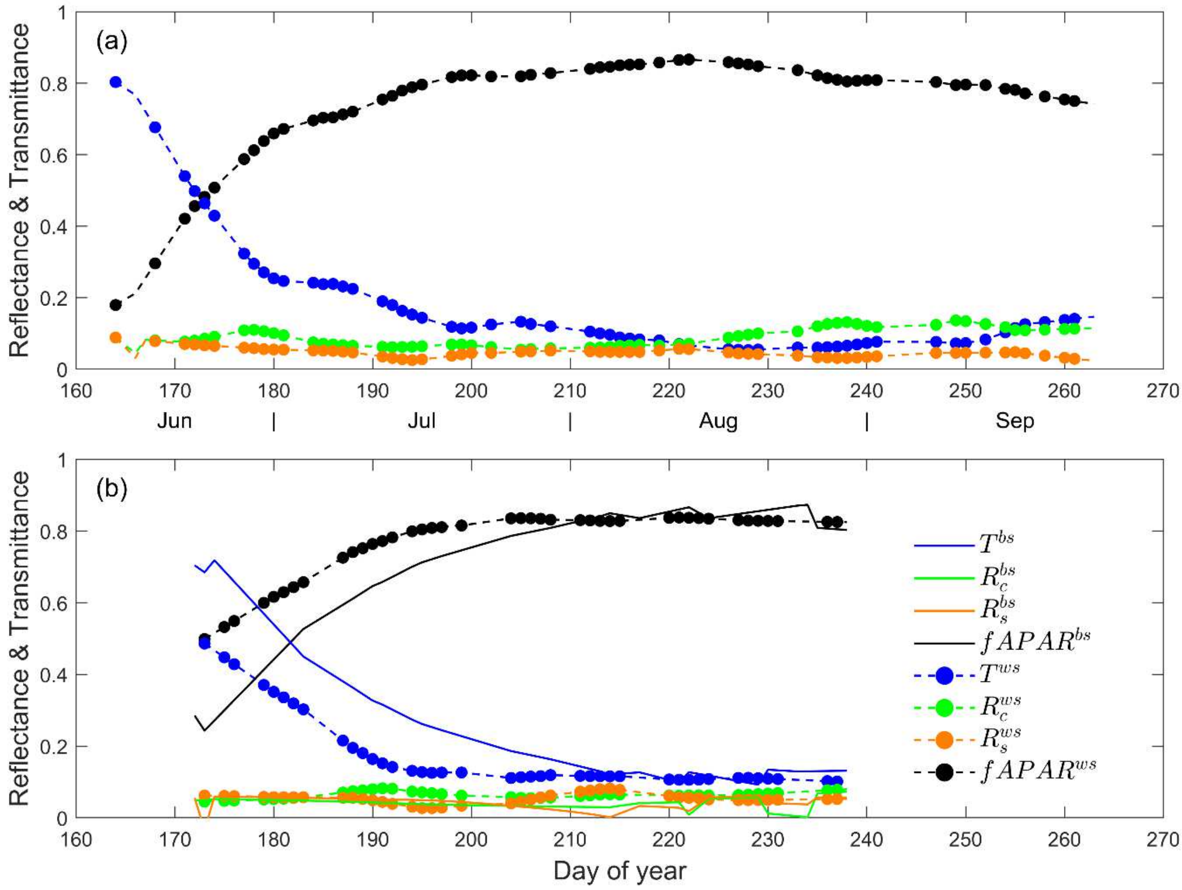

Fig. 3. Seasonal variation of canopy reflectance (R_c), soil reflectance (R_s), canopy transmittance (T), and fAPAR measured in 2012 (a) and 2013 (b) with AccuPAR. The solid and dashed lines represent the black-sky (with superscript $^{\text{'bs'}}$) and white-sky (with superscript $^{\text{'ws'}}$) conditions. The filled circles on lines represent the actual measurement days.

Our experimental results (Fig. 4) show that fAPAR_T(AccuPAR) estimated from the two-stream assumption (Eq. (5)) agrees very well with the reference four-stream fAPAR, fAPAR(AccuPAR) (Eq. (2)) under both black-sky and white-sky conditions (R^2 = 0.94~1, RMSE = 0.03~0.08). These two fAPAR quantities differ from less than 0.03 (4%) under black-sky conditions, the differences being larger when fAPAR(AccuPAR) is higher than 0.7 and under white-sky conditions.

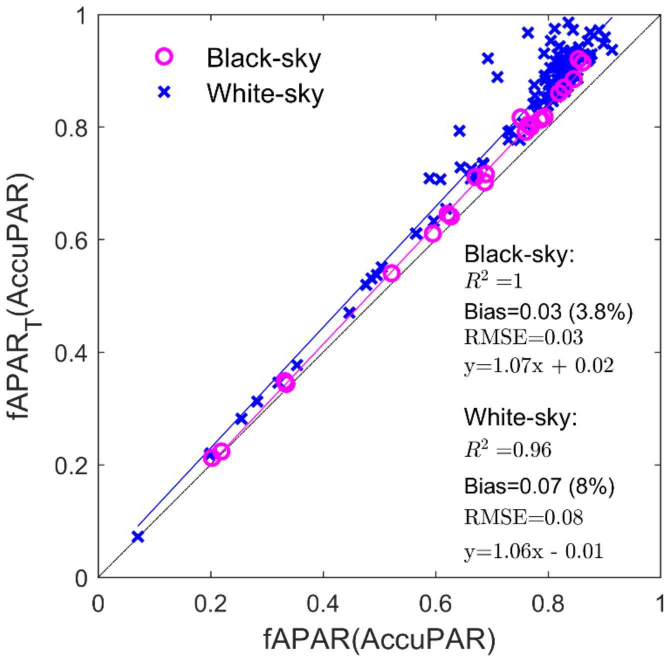

Fig. 4. Comparison of four-stream fAPAR(AccuPAR) (Eq. (2)) and the two-stream $fAPAR_T$ (AccuPAR)(Eq. (5)) values derived from AccuPAR measurements in 2012 and 2013 under both black (magenta) and white-sky (blue) conditions.

3.3 fAPAR and fIPAR of different instruments

White-sky fAPAR and fIPAR values rapidly increase until DOY 210 in 2012 and 2013 (Fig. 5). As expected, $fAPAR_T$(AccuPAR), fIPAR(DHP_{up}) and fIPAR(LAI-2200) and fAPAR (AccuPAR) are very close together during the entire season. Conversely, GfIPAR(DHP_{down}) is slightly higher than fAPAR(AccuPAR) during the early development stages and is much lower than the other quantities during the later stages: White-sky GfIPAR(DHP_{down}) decreases sharply after DOY 210. In contrast, the other quantities remain stable from DOY 210 to DOY 250 and slightly decrease after DOY 250. In 2013 where both black-sky and white-sky values were measured (Fig. 5b), the black-sky values are substantially smaller than the white-sky counterparts. However black-sky GfIPAR(DHP_{down}) is higher than the white-sky values at the end of the season (Fig. 5b).

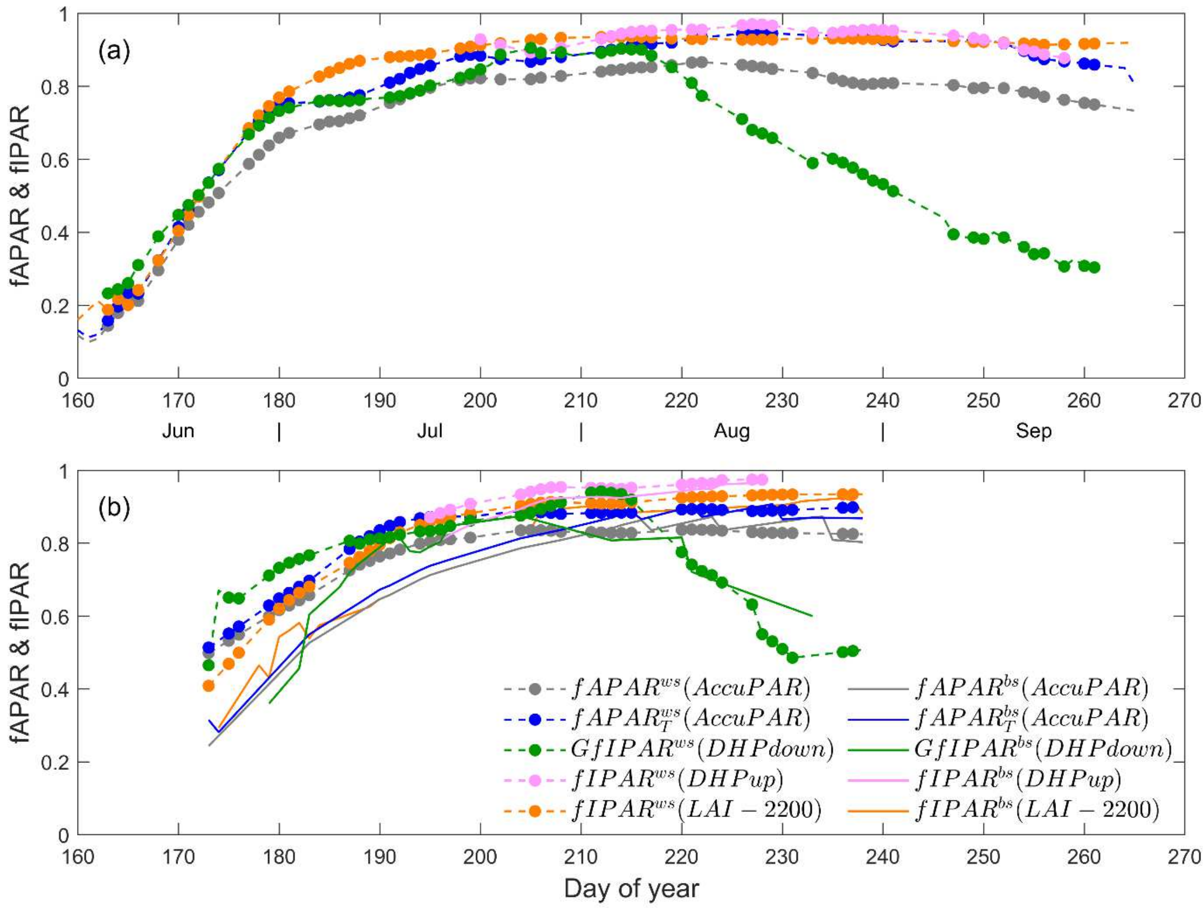

Fig. 5. Seasonal variation of fAPAR and fIPAR in 2012 (a) and 2013 (b). The solid and dashed lines represent the black-sky (with superscript 'bs') and white-sky (with superscript 'ws') conditions, respectively. In 2012, only white-sky conditions are presented.

We will focus here on the first growth period (before DOY 210) where senescence is marginal (Fig. 2) and GAI=PAI. As a consequence, GfAPAR=fAPAR and GfIPAR=fIPAR. We will therefore use here only the terms fAPAR and fIPAR except for GfIPAR(DHPdown) for which only the green elements are accessible (Table 1). The comparison between fAPAR and fIPAR will be made using $fAPAR_T$(AccuPAR) as a reference since we demonstrated previously that fAPAR(AccuPAR)≈0.96×$fAPAR_T$(AccuPAR) (Fig. 4).

GfIPAR(DHP_{down}) shows a high agreement with $fAPAR_T$(AccuPAR) under white-sky conditions (Fig. 6a) (R^2 = 0.82) with almost no bias. A strong correlation is also observed under black-sky conditions (Fig. 6a) with however a systematic overestimation (Bias=0.13). The correlation between $fAPAR_T$(AccuPAR) and the fIPAR(DHP_{up}) is weak both for the white-sky and black-sky values (Fig. 6b). fIPAR(LAI-2200) shows a high agreement with $fAPAR_T$(AccuPAR) (Fig. 6c), particularly under white-sky conditions.

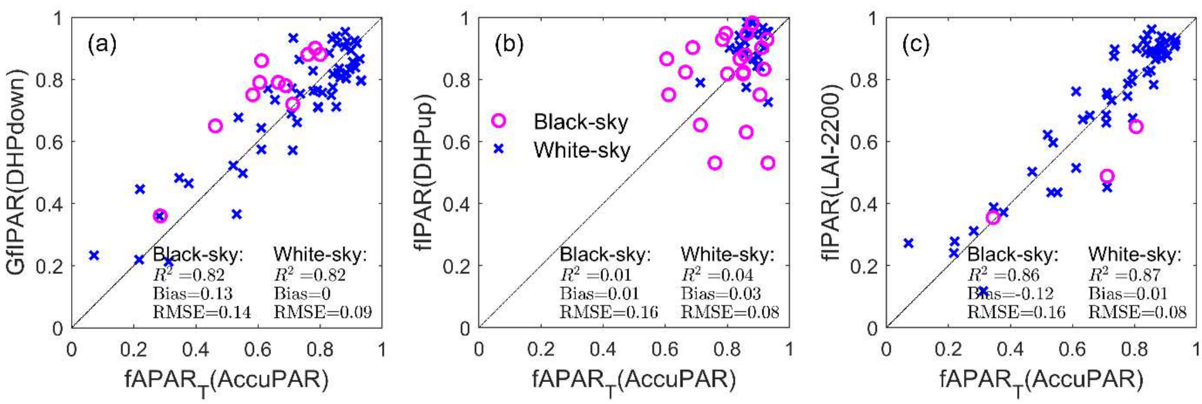

Fig. 6. Comparison between $fAPAR_T$(AccuPAR) used as a reference and GfIPAR(DHP_{down}), fIPAR(DHP_{up}) and fIPAR(LAI-2200). Data from the first period (before DOY 210) when no senescent elements are present. Black-sky (pink circles) and white-sky illumination conditions (blue crosses) are presented.

3.4 GfAPAR and GfIPAR during the senescence stage

We focus on the period starting after DOY 210 when senescence increases up to the maturity stage (Fig. 2). As a consequence, the GAI/PAI ratio decreases regularly with time (Fig. 7).

The canopy fAPAR measured by AccuPAR shows small variations due to saturation when PAI is generally higher than 4.0. Conversely, the green fIPAR derived from downward looking DHP, which can be taken as the best proxy of GfIPAR, decreases swiftly from 0.9 to 0.3 (Fig. 7). Assuming that green and non-green elements are mixed within the canopy (Viña and Gitelson, 2005), GfAPAR measured by AccuPAR (Eq. (15)) and GfIPAR measured by LAI-2200 (Eq. (17)) show a temporal profile close to the reference GfIPAR from downward looking DHP. Conversely, all green quantities derived with Chen (1996), (Eq. (14)) (e.g. assuming that the green elements are distributed at the top of canopy) are systematically higher than the reference GfIPAR from downward looking DHP. $GfIPAR^{mix}$ estimated from LAI-2200 and upward looking DHP are similar and higher than $GfAPAR^{mix}$ derived from AccuPAR.

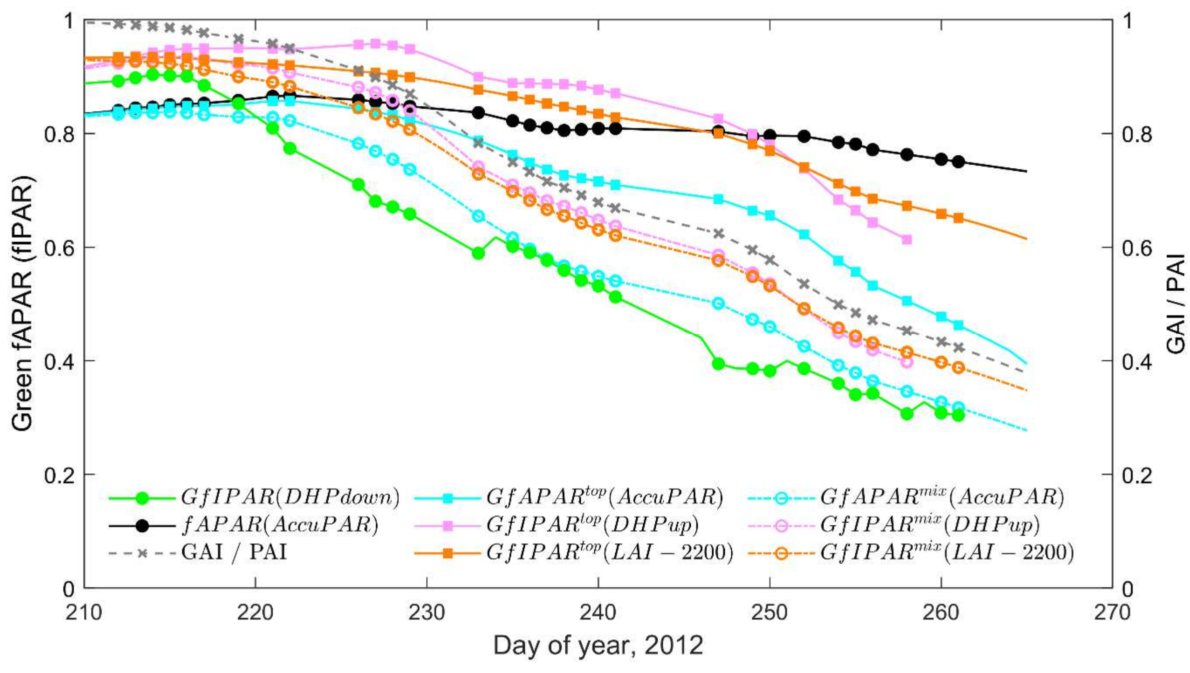

Fig. 7. Seasonal variation of fAPAR and fIPAR quantities considered in Table 1 during the senescent stage (after DOY 210). GAI/PAI is the ratio of GAI to PAI (right y-axis). All measurements were performed under white-sky illuminations in 2012.

Fig. 8 shows that GfAPAR(AccuPAR), GfIPAR(DHP_{up}) and GfIPAR(LAI-2200) are well correlated with GfIPAR(DHP_{down}) considered as the reference. However, significant biases are observed. Under the assumption that the green and non-green elements are mixed in the canopy (Viña and Gitelson, 2005, Eq. (15)), $GfAPAR^{mix}$(AccuPAR) is closer to the reference GfIPAR(DHP_{down}) (Bias = 0.02, Fig. 8a), while the $GfIPAR^{mix}$(DHP_{up}) and $GfIPAR^{mix}$(LAI-2200) are larger by around 0.1 (Fig. 8b and 8c). Conversely, assuming that the green elements are distributed at the top of canopy as proposed by Chen (1996), $GfAPAR^{top}$(AccuPAR), $GfIPAR^{top}$(DHP_{up}) and $GfIPAR^{top}$(LAI-2200) are systematically higher by 0.13 ~ 0.25 than reference GfIPAR(DHP_{down}).

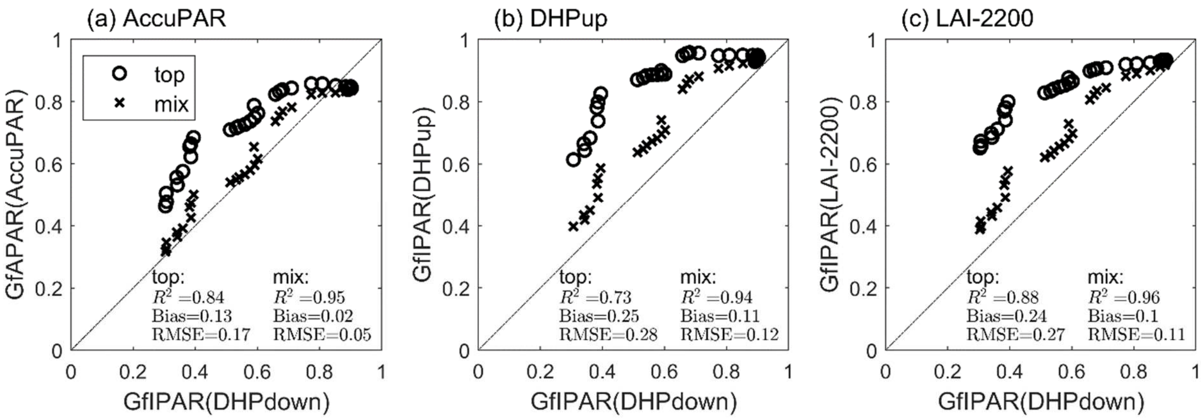

Fig. 8. After DOY 210 (senescence), from left to right: comparison of GfAPAR derived from AccuPAR, GfIPAR by upward DHP and LAI-2200 with the GfIPAR from downward DHP used as a reference. "top" and "mix" refers to the assumptions used to derive the green fAPAR, e.g. the senescence is occurring from the top of the canopy (Chen, 1996) or is randomly distributed within the canopy (Viña and Gitelson, 2005).

4 Discussion

4.1 Four-stream fAPAR versus two-stream $fAPAR_T$ estimation from AccuPAR

AccuPAR is appropriate to measure the fAPAR based on the four-stream approach (Eq. (2)). However, application of the four-stream assumption to compute fAPAR requires measuring simultaneously canopy reflectance and transmittance, together with the background reflectance. Measurement of the background reflectance is difficult since it requires setting the sensors close to the background which may disturb the canopy and influence the measurement. Furthermore, the spatial representativeness may also be an issue considering the high local spatial variability of the radiation field at the bottom of the canopy, due to the row spacing and canopy cover (Timlin et al., 2014). Conversely, the two-stream assumption (Eq. (5)) based on the sole measurement of canopy transmittance is appealing to estimate fAPAR.

The high consistency between fAPAR(AccuPAR) and $fAPAR_T$(AccuPAR) (Fig. 4) is mainly due to the small values of canopy and soil reflectance (Fig. 3). Furthermore, both terms are partly counterbalancing each other: in Eq. (2), canopy reflectance (R_c) varies between R_s for PAI=0 to $R\infty$ for very large PAI values. Conversely, the term T_{Rs} varies between R_s for PAI=0 to 0 for large PAI values. These experimental results are consistent with that of other studies (Gallo and Daughtry, 1986; Gobron et al., 2006; Gower et al., 1999; Kukal and Irmak, 2020). However, as shown by Eq. (4), the measured transmittance includes the contribution from multiple scattering between the bottom of the canopy and the ground, leading to an overestimation of the actual transmittance and thus on $fAPAR_T$ (Eklundh et al., 2011). Closer inspection of the values shows that $fAPAR_T$(AccuPAR) is systematically higher than fAPAR(AccuPAR), particularly for the well-developed canopies $fAPAR_T$(AccuPAR)≈1 when fAPAR(AccuPAR)≈1-R_∞≈0.96 as expected from Eq. (4) since R_∞≈0.04 (Fig. 3). We also computed the actual transmittance which is smaller than the measured one by -0.78% to -0.14% under cloudy conditions and -0.41% to -0.01% under clear sky conditions. Similarly, $fAPAR_T$ computed when considering multiple scattering is slightly larger than the $fAPAR_T$ we estimated by 0.22% to 3.3% under cloudy conditions and 0.2% to 3.09% under clear conditions. This small uncertainty is mainly due to low background reflectance of paddy rice. Nevertheless, higher uncertainties may occur for canopies with brighter backgrounds (Asner et al., 1998; Gower et al., 1999; Widlowski, 2010).

4.2 Comparison of fAPAR and fIPAR measured from different instruments during the green-up stage

The overestimations observed between $GfIPAR^{bs}(DHP_{down})$ and $fAPAR^{bs}$(AccuPAR) under black-sky conditions are mostly due to the limited spatial sampling when considering only the sun direction. In case of the black-sky conditions, AccuPAR measurements provide a better spatial sampling with the 80 sensors set along the 1 m long device. Conversely, for white-sky conditions, $GfIPAR^{ws}(DHP_{down})$ results from the integration of the black-sky values over all the directions (Eq. (10)) which provides to a much larger area sampled.

$fIPAR(DHP_{up})$ has a weak correlation with $fAPAR_T$(AccuPAR). This is mostly explained by the limited range of variation of $fAPAR_T$ points available. DHP measurements looking upward requires to set the camera at the bottom of the canopy. When the back of the camera is laying on the ground, the focal point of the lens is at about 16.5 cm above the ground. It is therefore not possible to use this technique for the early growth stages when the canopy is too short. This explains why no points are available for the low values of fAPAR or fIPAR (Fig.

6b). Further, only part of the vegetation elements are seen by the camera looking upward, resulting in possible underestimation of fIPAR(DHP_{up}). In addition, setting the camera on the ground disturbs canopy architecture and may also bias the spatial sampling since it is not possible to set the camera at the position of the row. Finally, the area sampled by the camera looking upward from the bottom of the canopy is lower than in the case of fIPAR(DHP_{down}): the distance between the camera and the top of the canopy (upward looking DHP) is shorter than the distance from the camera to the ground (downward looking DHP). This explains why significant scattering of data is observed between fIPAR(DHP_{up}) and $fAPAR_T$(AccuPAR). It is therefore recommended to use a very small camera and to improve the spatial sampling by taking more images. Nevertheless, fIPAR(DHP_{up}) should be used mostly for relatively high and sparse canopies such as maize crops to limit both the disturbances when taking the pictures and the parts not sampled at the bottom of the canopy because of the height of the lens above the ground.

The small discrepancies observed between both quantities demonstrate that the spatial sampling was sufficient for LAI-2200 (8 points per ESU), although more limited than that of the AccuPAR (4 readings of the 80 PAR sensors set along the 1m probe). Under black-sky conditions, only three matching pairs were available because the LAI-2200 was only performed under cloudy conditions and the large sun zenith angles prevent the black-sky $fIPAR^{bs}$(LAI-2200) calculations.

Among the three methods investigated (DHP_{down}, DHP_{up} and LAI2200), DHP_{down} shows obvious advantages: it provides a good agreement with $fAPAR_T$, while not disturbing canopy architecture since the camera is placed above the canopy. However, in the case of deriving black-sky fIPAR values, more samples should be taken to compensate the small footprint of the camera in the sun direction. Further, great care should be taken when segmenting the image which is more difficult and uncertain for dense canopies and sunny illumination conditions (Garrigues et al., 2008). Indeed, more advanced classification method is necessary to improve the DHP data processing (Duveiller and Defourny, 2010; Jonckheere et al., 2017).

4.3 Impacts of illumination conditions on fAPAR and fIPAR estimations

fAPAR and fIPAR present diurnal variations due to variations of the solar zenith angle and the proportion of diffuse PAR in the total downwelling radiation. These variations have a significant impact on the photosynthetic efficiency and on the canopy light regime (Aikman, 1989; Grant, 1999; Wang et al., 2006). We therefore compared the ability of instruments to retrieve the black-sky and white-sky fAPAR components. Our results show that instantaneous fAPAR and fIPAR under white-sky conditions are slightly higher than under black-sky conditions, which is consistent with previous results based on both model simulation and ground measurements (Li and Fang, 2015; Nouvellon, 2000; Thomas et al., 2006). The resulting daily integrated fAPAR can be more or less affected depending on the variation of the diffuse PAR fraction throughout the day. Therefore, except for AccuPAR, accurate daily fAPAR estimation requires auxiliary measurements of the PAR diffuse fraction or specific development such as proposed by Hanan and Bégué (1995) for LAI-2200.

4.4 Estimations of green fAPAR and fIPAR during the senescence period

During the senescence period, both green and senescent elements contribute to fAPAR at the canopy level (Asner et al., 1998; Di Bella et al., 2004; Huemmrich et al., 2005; Rahman et al., 2019). Since only the green components are used for photosynthesis and transpiration, the green fAPAR should be the quantity to be considered. Downward DHP is the only method that provides a direct estimate of green fIPAR because it minimizes problems due to senescent elements generally located at the bottom of the canopy (Baret et al., 2010). Green fIPAR from downward DHP is therefore used as the reference method. Conversely, the green fAPAR cannot be directly measured by the other methods since the instruments are looking from the bottom of the canopy and green and non-green components cannot be easily distinguished. We evaluated two methods to derive green fAPAR or green fIPAR from canopy fAPAR and fIPAR measured quantities using the GAI/PAI ratio, based on different assumptions on the spatial distribution of green and non-green elements. In paddy rice crops, the senescence happens right after the ear appearance, and is observed at leaf tips and at the bottom of the canopy. The ears, distributed mainly at the top layer and mixed with green leaves, become yellow and brown, and the senescent leaves at the bottom layer grow upward and mix with other green stems and leaves. This behavior is thus closer to the random mixing hypothesis of Viña and Gitelson (2005) than to the Chen (1996) assumption that green elements are concentrated in the top layer. However, these two correction methods developed to get the green fAPAR or fIPAR from the canopy fAPAR or fIPAR requires the measurement of the GAI/PAI ratio during the senescence period.

5 Conclusion

The main objective of this study was to compare several methods and instruments for fAPAR or fIPAR estimates over paddy rice and investigate the impact of canopy senescence under different illumination conditions. Results showed that using only canopy transmittance ($fAPAR_T$(AccuPAR)) measured by AccuPAR provides a good proxy of the four-stream reference fAPAR(AccuPAR). This allows to simplify the AccuPAR measurements over paddy rice fields while keeping a high degree of accuracy.

Canopy transmittance can also be measured using DHP looking upward or downward and LAI-2200, resulting respectively into fIPAR(DHP_{up}), GfIPAR(DHP_{down}) and fIPAR(LAI2200). Our results demonstrated that fIPAR(DHP_{up}) was leading to uncertainties mostly because of the dimensions of the camera used, disturbing canopy architecture when placed at the bottom of the crop and missing also a significant fraction of the vegetation elements located below the lens of the camera. For these reasons, downward looking DHP (GfIPAR(DHP_{down})), AccuPAR ($fAPAR_T$(AccuPAR)) and LAI-2200 (fIPAR(LAI-2200)) are better suited for rice crops that are dense and relatively short. However, the spatial sampling should be adapted to the actual footprint of each instrument. Three AccuPAR, four LAI-2200 or 15 to 20 DHPs seems sufficient to get precise estimates of white-sky fAPAR or fIPAR over an area of ≈100m² of homogeneous rice crops. This minimum sampling appears also sufficient under black-sky conditions, except for DHPs for which the footprint is very small in the sun direction. To avoid taking more images in order to improve the area sampled, it is advised to integrate canopy transmittance over all the compass directions as done for LAI-2200. Nevertheless, the daily integrated green fAPAR and fIPAR are required in many vegetation functional models (Baret and Guyot, 1991; Gower et al., 1999; Weiss et al., 2007). The daily integrated fAPAR and fIPAR values can be derived from the DHP images, which will also result in a much larger area sampled. Note that DHPs appear the best suited method to estimate daily variation and daily integrated values of fIPAR since a single image taken during the day allows to derive canopy transmittance for all possible incoming light directions, assuming that canopy architecture keeps stable during the day. This assumption seems reasonable for rice crops, but not realistic for heliotropic species and species presenting leaf rolling reaction to water stresses (Baret et al., 2018).

Downward looking DHPs is the only method that measures directly GfIPAR, the fraction of incoming light intercepted by the green photosynthetically active parts of the vegetation. This offers a great advantage over the other instruments when a significant part of the organs are senescing as observed over rice crops after flowering. AccuPAR and LAI-2200 are measuring canopy transmittance from the bottom of the canopy and are not able to distinguish between the green and non-green parts. Corrections are proposed for these instruments, based on independent measurement of the GAI/PAI ratio. Measuring the GAI/PAI ratio is generally done by destructive methods, which is laborious, time consuming, and not well suited for crop monitoring. Further, the corrections need assumptions on the vertical distribution of the senescing parts. For rice crops, we demonstrated that the method proposed by Viña and Gitelson (2005), assuming that green and non-green elements are well mixed, provides the best agreement with GfIPAR(DHP_{down}) considered as the reference method.

Downward looking DHPs appears thus to be the best method to estimate GfIPAR under relatively short canopies. It is currently used intensively over a number of crops (Camacho et al., 2013; Li et al., 2015; Weiss et al., 2007). For taller canopies that prevents easy characterization from the top, $fAPAR_T$(AccuPAR), fIPAR(DHPup) and fIPAR(LAI-2200) should be preferred. Exploitation of DHPs requires images with good resolution and acquired under favorable illumination conditions. As a matter of facts, sunny conditions are not ideal since the distinction between green and non-green parts (background and senescent elements) is difficult in the shadows because of the small dynamics of the pixel values as well as in the specularly reflected areas where colors are lost. Using HDR (High Dynamic Range) features and applying a gamma factor should partly solve the problem. Nevertheless, image segmentation to identify the green pixels is still not fully automatic which is the main limitation of the DHP downward looking method as compared to AccuPAR and LAI-2200. Additional work is therefore required to develop algorithms capable of identifying automatically the green pixels in the images with a high degree of accuracy.

6 Acknowledgements

This study was supported by the National Natural Science Foundation of China (41171333, H.F.). We would like to thank the local farmers for allowing us to take experiment on their fields and the students who helped in the field campaigns in 2012 and 2013. We also would like to thank Dr. Chongya Jiang and Dr. Tao Sun in the preparation of field measurements. Anonymous reviewers are thanked for valuable comments.

7 Appendix A. Rice field pictures during growing season

Fig. A1. Rice field pictures of Plot B from end of July to September, 2012.

8 References

Aikman, D.P., 1989. Potential Increase in Photosynthetic Efficiency from the Redistribution of Solar Radiation in a Crop. J Exp Bot 40, 855–864. https://doi.org/10.1093/jxb/40.8.855

Asner, G.P., Wessman, C.A., Archer, S., 1998. Scale Dependence of Absorption of Photosynthetically Active Radiation in Terrestrial Ecosystems. Ecological Applications 8, 1003–1021.

Baret, F., Andrieu, B., Steven, M., 1993. Gap frequency and canopy architecture of sugar beet and wheat crops. Agricultural and Forest Meteorology 65, 261–279. https://doi.org/10.1016/0168-1923(93)90008-6

Baret, F., de Solan, B., Lopez-Lozano, R., Ma, K., Weiss, M., 2010. GAI estimates of row crops from downward looking digital photos taken perpendicular to rows at 57.5° zenith angle: Theoretical considerations based on 3D architecture models and application to wheat crops. Agricultural and Forest Meteorology 150, 1393–1401. https://doi.org/10.1016/j.agrformet.2010.04.011

Baret, F., Guyot, G., 1991. Potentials and limits of vegetation indices for LAI and APAR assessment. Remote Sensing of Environment 35, 161–173. https://doi.org/10.1016/0034-4257(91)90009-U

Baret, F., Madec, S., Irfan, K., Lopez, J., Comar, A., Hemmerlé, M., Dutartre, D., Praud, S., Tixier, M.H., 2018. Leaf-rolling in maize crops: from leaf scoring to canopy-level measurements for phenotyping. Journal of Experimental Botany 69, 2705–2716. https://doi.org/10.1093/jxb/ery071

Camacho, F., Cernicharo, J., Lacaze, R., Baret, F., Weiss, M., 2013. GEOV1: LAI, FAPAR essential climate variables and FCOVER global time series capitalizing over existing products. Part 2: Validation and intercomparison with reference products. Remote Sensing of Environment 137, 310–329. https://doi.org/10.1016/j.rse.2013.02.030

Campos, I., Neale, C.M.U., Calera, A., 2017. Is row orientation a determinant factor for radiation interception in row vineyards?: Row direction influences light capture in vineyard. Australian Journal of Grape and Wine Research 23, 77–86. https://doi.org/10.1111/ajgw.12246

Chen, J., 1996. Canopy Architecture and Remote Sensing of the Fraction of Photosynthetically Active Radiation Absorbed by Boreal Conifer Forests. IEEE Transactions on Geoscience and Remote Sensing 34, 1353–1368.

Cohen, S., Rao, R.S., Cohen, Y., 1997. Canopy transmittance inversion using a line quantum probe for a row crop. Agricultural and Forest Meteorology 86, 225–234.

Decagon Devices, 2010. AccuPAR PAR/LAI ceptometer model LP-80 Operator's Manual Version 10 [WWW Document]. URL http://www.cen.ulaval.ca/nordicanad/donnees/n_45561/v582105/file/supp/Decagon_Accupar_LP80_Web.pdf

Demarez, V., Duthoit, S., Baret, F., Weiss, M., Dedieu, G., 2008. Estimation of leaf area and clumping indexes of crops with hemispherical photographs. Agricultural and Forest Meteorology 148, 644–655. https://doi.org/10.1016/j.agrformet.2007.11.015

Di Bella, C.M., Paruelo, J.M., Becerra, J.E., Bacour, C., Baret, F., 2004. Effect of senescent leaves on NDVI-based estimates of *f* APAR: Experimental and modelling evidences. International Journal of Remote Sensing 25, 5415–5427. https://doi.org/10.1080/01431160412331269724

Duveiller, G., Defourny, P., 2010. Batch processing of hemispherical photography using object-based image analysis to derive canopy biophysical variables. Presented at the GEOBIA 2010-Geographic Object-Based Image Analysis, Ghent University, Ghent, Belgium, p. 5.

Eklundh, L., Jin, H., Schubert, P., Guzinski, R., Heliasz, M., 2011. An Optical Sensor Network for Vegetation Phenology Monitoring and Satellite Data Calibration. Sensors 11, 7678–7709. https://doi.org/10.3390/s110807678

Fang, H., Li, W., Wei, S., Jiang, C., 2014a. Seasonal variation of leaf area index (LAI) over paddy rice fields in NE China: Intercomparison of destructive sampling, LAI-2200, digital hemispherical photography (DHP), and AccuPAR methods. Agricultural and Forest Meteorology 198–199, 126–141. https://doi.org/10.1016/j.agrformet.2014.08.005

Fang, H., Li, W., Wei, S., Sun, T., Jiang, C., 2014b. Paddy Rice Experiment in the Sanjiang Plain (PRESP) Field Measurement Report. Institute of Geographic Sciences and Natural Resources Research, Chinese Academy of Sciences, Beijing, China.

Fang, H., Ye, Y., Liu, W., Wei, S., Ma, L., 2018. Continuous estimation of canopy leaf area index (LAI) and clumping index over broadleaf crop fields: An investigation of the PASTIS-57 instrument and smartphone applications. Agricultural and Forest Meteorology 253–254, 48–61. https://doi.org/10.1016/j.agrformet.2018.02.003

Fensholt, R., Sandholt, I., Rasmussen, M.S., 2004. Evaluation of MODIS LAI, fAPAR and the relation between fAPAR and NDVI in a semi-arid environment using in situ measurements. Remote Sensing of Environment 91, 490–507. https://doi.org/10.1016/j.rse.2004.04.009

Gallo, K.P., Daughtry, C.S.T., 1986. Techniques for Measuring Intercepted and Absorbed Photosynthetically Active Radiation in Corn Canopies [1]. Agron. J. 78, 752–756. https://doi.org/10.2134/agronj1986.00021962007800040039x

Garrigues, S., Shabanov, N.V., Swanson, K., Morisette, J.T., Baret, F., Myneni, R.B., 2008. Intercomparison and sensitivity analysis of Leaf Area Index retrievals from LAI-2000, AccuPAR, and digital hemispherical photography over croplands. Agricultural and Forest Meteorology 148, 1193–1209. https://doi.org/10.1016/j.agrformet.2008.02.014

GCOS, 2016. The Global Observing System for Climate: Implementation Needs (GCOS- 200). World Meteorological Organization.

Gobron, N., Pinty, B., Aussedat, O., Chen, J.M., Cohen, W.B., Fensholt, R., Gond, V., Huemmrich, K.F., Lavergne, T., Mélin, F., Privette, J.L., Sandholt, I., Taberner, M., Turner, D.P., Verstraete, M.M., Widlowski, J.-L., 2006. Evaluation of fraction of absorbed photosynthetically active radiation products for different canopy radiation transfer regimes: Methodology and results using Joint Research Center products derived from SeaWiFS against ground-based estimations. J. Geophys. Res. 111, D13110. https://doi.org/10.1029/2005JD006511

Goward, S.N., Huemmrich, K.E., 1992. Vegetation Canopy PAR Absorptance and the Normalized Difference Vegetation Index: An Assessment Using the SAIL Model. Remote Sensing of Environment 39, 119–140.

Gower, S.T., Kucharik, C.J., Norman, J.M., 1999. Direct and Indirect Estimation of Leaf Area Index, fAPAR, and Net Primary Production of Terrestrial Ecosystems. Remote Sensing of Environment 70, 29–51. https://doi.org/10.1016/S0034-4257(99)00056-5

Grant, R.H., 1999. Ultraviolet-B and photosynthetically active radiation environment of inclined leaf surfaces in a maize canopy and implications for modeling. Agricultural and Forest Meteorology 95, 187–201. https://doi.org/10.1016/S0168-1923(99)00023-4

Gu, L., Baldocchi, D., Verma, S.B., Black, T.A., Vesala, T., Falge, E.M., Dowty, P.R., 2002. Advantages of diffuse radiation for terrestrial ecosystem productivity: advantages of diffuse radiation. J. Geophys. Res. 107, ACL 2-1-ACL 2-23. https://doi.org/10.1029/2001JD001242

Hanan, N.P., Bégué, A., 1995. A method to estimate instantaneous and daily intercepted photosynthetically active radiation using a hemispherical sensor. Agricultural and Forest Meteorology 74, 155–168. https://doi.org/10.1016/0168-1923(94)02196-Q

Huemmrich, K.F., Privette, J.L., Mukelabai, M., Myneni, R.B., Knyazikhin, Y., 2005. Time-series validation of MODIS land biophysical products in a Kalahari woodland, Africa. International Journal of Remote Sensing 26, 4381–4398. https://doi.org/10.1080/01431160500113393

Jonckheere, I.G.C., Macfarlane, C., Walter, J.-M.N., 2017. Image Analysis of Hemispherical Photographs, Algorithms and Calculations, in: Hemispherical Photography in Forest Science: Theory, Methods, Applications. Springer Netherlands, Dordrecht, pp. 115–151.

Jongschaap, R.E.E., Dueck, T.A., Marissen, N., Hemming, S., Marcelis, L.F.M., 2006. Simulating seasonal patterns of increased greenhouse crop production by conversion of direct radiation into diffuse radiation. Acta Hortic. 315–322. https://doi.org/10.17660/ActaHortic.2006.718.36

Kobayashi, H., Ryu, Y., Baldocchi, D.D., Welles, J.M., Norman, J.M., 2013. On the correct estimation of gap fraction: How to remove scattered radiation in gap fraction measurements? Agricultural and Forest Meteorology 174–175, 170–183. https://doi.org/10.1016/j.agrformet.2013.02.013

Kukal, M.S., Irmak, S., 2020. Light interactions, use and efficiency in row crop canopies under optimal growth conditions. Agricultural and Forest Meteorology 284, 107887. https://doi.org/10.1016/j.agrformet.2019.107887

Leblanc, S.G., Chen, J.M., 2001. A practical scheme for correcting multiple scattering effects on optical LAI measurements. Agricultural and Forest Meteorology 15.

Leblanc, S.G., Chen, J.M., Fernandes, R., Deering, D.W., Conley, A., 2005. Methodology comparison for canopy structure parameters extraction from digital hemispherical photography in boreal forests. Agricultural and Forest Meteorology 129, 187–207. https://doi.org/10.1016/j.agrformet.2004.09.006

Li, W., Fang, H., 2015. Estimation of direct, diffuse, and total FPARs from Landsat surface reflectance data and ground-based estimates over six FLUXNET sites: Landsat direct, diffuse and total FPARs. J. Geophys. Res. Biogeosci. 120, 96–112. https://doi.org/10.1002/2014JG002754

Li, W., Weiss, M., Waldner, F., Defourny, P., Demarez, V., Morin, D., Hagolle, O., Baret, F., 2015. A generic algorithm to estimate LAI, FAPAR and FCOVER variables from SPOT4_HRVIR and Landsat sensors: Evaluation of the consistency and comparison with ground measurements. Remote Sensing 7, 15494–15516.

Lizaso, J.I., Batchelor, W.D., Boote, K.J., Westgate, M.E., Rochette, P., Moreno-Sotomayor, A., 2005. Evaluating a Leaf-Level Canopy Assimilation Model Linked to CERES-Maize. Agron. J. 97, 734–740. https://doi.org/10.2134/agronj2004.0172

Martonchik, J.V., Bruegge, C.J., Strahler, A.H., 2000. A review of reflectance nomenclature used in remote sensing. Remote Sensing Reviews 19, 9–20. https://doi.org/10.1080/02757250009532407

McCallum, I., Wagner, W., Schmullius, C., Shvidenko, A., Obersteiner, M., Fritz, S., Nilsson, S., 2010. Comparison of four global FAPAR datasets over Northern Eurasia for the year 2000. Remote Sensing of Environment 114, 941–949. https://doi.org/10.1016/j.rse.2009.12.009

Monteith, J.L., 2015. Light Interception and Radiative Exchange in Crop Stands, in: Eastin, J.D., Haskins, F.A., Sullivan, C.Y., van Bavel, C.H.M. (Eds.), Physiological Aspects of Crop Yield. American Society of Agronomy, Crop Science Society of America, Madison, WI, USA, pp. 89–111. https://doi.org/10.2135/1969.physiologicalaspects.c9

Nilson, T., 1971. A theoretical analysis of the frequency of gaps in plant stands. Agricultural Meteorology 8, 25–38. https://doi.org/10.1016/0002-1571(71)90092-6

Nouvellon, Y., 2000. PAR extinction in shortgrass ecosystems: effects of clumping, sky conditions and soil albedo. Agricultural and Forest Meteorology 105, 21–41. https://doi.org/10.1016/S0168-1923(00)00194-5

Pinter, P.J., 1993. Solar angle independence in the relationship between absorbed PAR and remotely sensed data for alfalfa. Remote Sensing of Environment 46, 19–25. https://doi.org/10.1016/0034-4257(93)90029-W

Rahman, M.M., Lamb, D.W., Samborski, S.M., 2019. Reducing the influence of solar illumination angle when using active optical sensor derived NDVIAOS to infer fAPAR for spring wheat (Triticum aestivum L.). Computers and Electronics in Agriculture 156, 1–9. https://doi.org/10.1016/j.compag.2018.11.007

Rahman, M.M., Lamb, D.W., Stanley, J.N., 2015. The impact of solar illumination angle when using active optical sensing of NDVI to infer fAPAR in a pasture canopy. Agricultural and Forest Meteorology 202, 39–43. https://doi.org/10.1016/j.agrformet.2014.12.001

Senna, M.C.A., 2005. Fraction of photosynthetically active radiation absorbed by Amazon tropical forest: A comparison of field measurements, modeling, and remote sensing. J. Geophys. Res. 110, G01008. https://doi.org/10.1029/2004JG000005

Steinberg, D.C., Goetz, S.J., Hyer, E.J., 2006. Validation of MODIS F/sub PAR/ products in boreal forests of Alaska. IEEE Trans. Geosci. Remote Sensing 44, 1818–1828. https://doi.org/10.1109/TGRS.2005.862266

Thomas, V., Finch, D.A., McCaughey, J.H., Noland, T., Rich, L., Treitz, P., 2006. Spatial modelling of the fraction of photosynthetically active radiation absorbed by a boreal mixedwood forest using a lidar–hyperspectral approach. Agricultural and Forest Meteorology 140, 287–307. https://doi.org/10.1016/j.agrformet.2006.04.008

Timlin, D.J., Fleisher, D.H., Kemanian, A.R., Reddy, V.R., 2014. Plant Density and Leaf Area Index Effects on the Distribution of Light Transmittance to the Soil Surface in Maize. Agronomy Journal 106, 1828–1837. https://doi.org/10.2134/agronj14.0160

Viña, A., Gitelson, A.A., 2005. New developments in the remote estimation of the fraction of absorbed photosynthetically active radiation in crops: REMOTE ESTIMATION OF FAPAR IN CROPS. Geophys. Res. Lett. 32. https://doi.org/10.1029/2005GL023647

Wang, Xiping, Guo, Y., Li, B., Wang, Xiyong, Ma, Y., 2006. Evaluating a three dimensional model of diffuse photosynthetically active radiation in maize canopies. Int J Biometeorol 50, 349–357. https://doi.org/10.1007/s00484-006-0032-0

Weiss, M., Baret, F., 2010. CAN-EYE V6.1 user manual [WWW Document]. URL https://www6.paca.inrae.fr/can-eye

Weiss, M., Baret, F., Garrigues, S., Lacaze, R., 2007. LAI and fAPAR CYCLOPES global products derived from VEGETATION. Part 2: validation and comparison with MODIS collection 4 products. Remote Sensing of Environment 110, 317–331. https://doi.org/10.1016/j.rse.2007.03.001

Weiss, M., Baret, F., Li, W., Fang, H., 2018. Differences in FAPAR definitions for the validation of satellite products against ground measurements. Presented at the Workshop on Land Product Validation and Evolution.

Widlowski, J.-L., 2010. On the bias of instantaneous FAPAR estimates in open-canopy forests. Agricultural and Forest Meteorology 150, 1501–1522. https://doi.org/10.1016/j.agrformet.2010.07.011

Xiao, X., 2004. Modeling gross primary production of temperate deciduous broadleaf forest using satellite images and climate data. Remote Sensing of Environment 91, 256–270. https://doi.org/10.1016/j.rse.2004.03.010

Ye, M., Cao, Z., Yu, Z., Bai, X., 2015. Crop feature extraction from images with probabilistic superpixel Markov random field. Computers and Electronics in Agriculture 114, 247–260. https://doi.org/10.1016/j.compag.2015.04.010

Zhang, Q., Xiao, X., Braswell, B., Linder, E., Baret, F., Mooreiii, B., 2005. Estimating light absorption by chlorophyll, leaf and canopy in a deciduous broadleaf forest using MODIS data and a radiative transfer model. Remote Sensing of Environment 99, 357–371. https://doi.org/10.1016/j.rse.2005.09.009

Zhao, L., Liu, Z., Xu, S., He, X., Ni, Z., Zhao, H., Ren, S., 2018. Retrieving the Diurnal FPAR of a Maize Canopy from the Jointing Stage to the Tasseling Stage with Vegetation Indices under Different Water Stresses and Light Conditions. Sensors 18, 3965. https://doi.org/10.3390/s18113965

Zhong, W.W., Liu, J.Q., Zhou, X.B., Chen, Y.H., Bi, J.J., 2015. Row spacing and irrigation effect on radiation use efficiency of winter wheat. J. Anim. Plant Sci. 25, 448–455.